

PO-AK

Amstutz

RU 205

5143

High rates of bedload transport measured from **infilling** rate of large
strudel-scour craters in the Beaufort Sea, Alaska

Erk Reimnitz and E. W. Kempema

U.S. Geological Survey
345 Middlefield Road
Menlo Park, California 94025

Final version after acceptance by journal
is returned to Chickone on 8-30-82.

High rates of **bedload** transport measured from **infilling** rate of large **strudel-scour** craters in the **Beaufort** Sea, Alaska

By: Erk Reimnitz and Edward W. **Kempema**, U. S. Geological Survey,
345 Middlefield Road, Menlo Park, California 94025

ABSTRACT

Strudel scours are craters in the sea floor as much as 25 m wide and 6 m deep, that are excavated by vertical drainage flow during the **yearly** spring flooding of vast reaches of shorefast ice surrounding arctic deltas; they form at a rate of about $2.5 \text{ km}^2 \text{ yr}^{-1}$. We monitored **two** such craters in the Beaufort Sea and found that in relatively unprotected sites they fill in by deposition from bedload in 2 to 3 years. Net westward sediment transport results in sand layers dipping at the angle of repose westward into the strudel-scour crater, **whereas** the west **wall of** the crater remains steep to vertical. At the very bottom the crater traps almost all bedload: sand, pebbles, and organic detritus. As **infilling** progresses, the materials are increasingly **winnowed**, and bypassing must occur. Over a 20-m-wide sector, an exposed strudel scour trapped 360 m^3 of bedload during **two** seasons; this **infilling** represents a bedload transport rate of $9 \text{ m}^3 \text{ yr}^{-1} \text{ m}^{-1}$. This rate should be applicable to a 4.5-km-wide zone with equal exposure and similar or **shallower** depth. Within this zone, the transport rate is $40,500 \text{ m}^3 \text{ yr}^{-1}$, similar to estimated **longshore** transport rates on **local** barrier beaches. Based on of the established rate of cut and fill, all the delta-front deposits should consist of strudel-scour fill. **Vibrocoring** typically show dipping interbedded sand and lenses of organic material draped over very steep erosional contacts, and an absence of horizontal continuity of strata--criteria that should uniquely identify high-latitude **deltaic** deposits. Given a short **2-** to 3-year lifespan, most strudel scours seen in surveys must be old

and partially filled. The same holds true for ice gouges and other depressions not adjusted to summer waves and currents, and therefore such features record events of only the past few years. In view of such high rates of bottom **reworking** of the shallow shelf, any human activities causing turbidity, such as dredging, **would** have little effect on the environment. However, huge amounts of transitory material trapped by long causeways planned for offshore development **would** result in major changes in the environment.

INTRODUCTION

The yearly spring flooding of vast expanses of shorefast ice on the inner shelf in the Arctic, and the commonly violent draining of these floodwaters through the ice, result in the formation of large scour craters called strudel scours. Strudel scours, and their subsequent sediment fill, are important erosional and **depositional** features of high-latitude **deltaic** environments (REIMNITZ, et al., 1974). Recognition of these features may serve as a criterion for identifying similar paleoenvironments. Industry considers strudel scours to be one of the most serious geologic hazards to pipelines on **shallow-shelf** areas affected by the phenomenon (L. J. Toimil, oral communication, 1981). The purpose of this report is to present data and observations on the **infilling** rate of **two** strudel scours in diverse environments of the shallow Beaufort Sea shelf near **Prudhoe Bay**, Alaska. Both scours were similar in size, with lips at 2.5-m **water** depth, but one was sheltered by a nearby barrier island, **whereas** the other was located on an exposed prodelta.

A comparison of the measured rapid rate of strudel-scour excavation and **infilling** with the generally slow rate of delta accretion in arctic regions

demonstrates strudel-scour fill as an important compositional component of prodeltas. We present strong evidence that this strudel-scour fill consists of materials supplied almost entirely by bedload transport. **Thus,** the rate of **infilling allows** calculations of bedload transport rates that probably are more reliable than those that could be obtained by any other means known to us. Among the requirements for an efficient **bedload** transport sampler (Hubbell, 1964) are the following:

- (1) it is very large compared to seabed relief, and therefore gives a good average,
- (2) it should **not** alter **bedload** discharge by changing **local** flow patterns,
- (3) it **should collect** the largest as **well** as the smallest **bedload** particles,
- (4) it should give **all** particles an **equal** opportunity for entrance, regardless of size and direction of movement,
- (5) sampler is stable, and
- (6) sampling period is long relative to period of changing hydraulic conditions.

As the strudel scours monitored meet these requirements better than most man-made devices, the **bedload** transport rates determined from this study should be close to actual rates of transport.

BACKGROUND INFORMATION

Wave and current **reworking** of the inner-shelf surface is restricted to the short open-water season starting in July and extending to the onset of freezeup in late September to early October. Current-meter records from November to January show maximum flow velocities decreasing from 10- to less than 2-cm s⁻¹ (MATTHEWS, 1981). Diving observations made under the ice during the winter revealed only very **low** current velocities. Under-ice current

- observations made during the time and within the area of overflow are too sketchy to indicate whether **reworking** of bottom sediment occurs during overflow. Currents do not increase noticeably until about mid-July, **when** the ice breaks up (BARNES, 1982). The rivers of northern Alaska begin carrying water to the sea by the end of May or early June, **when** the fast ice is 1.7 to 2 m thick and still intact. This ice is inundated by 0.5 to 1.5 m of fresh water for distances of as much as 15 km or even more from the river mouths (REIMNITZ and BRUDER, 1972; REIMNITZ et al., 1974; WALKER, 1974). Figure 1 shows a part of the Beaufort Sea shelf in the vicinity of the Prudhoe Bay oilfields at a time **when** those rivers with **headwaters** in the Brooks Range are beginning to flow, while those with drainage basins entirely within the coastal plain are still dormant.

When the coastal-plain drainage systems thaw and the flooding is at its maximum, the inundated ice areas may nearly merge, **especially** between the Colville and Kuparuk Rivers. Within a few days, however, most of the floodwaters drain off the ice. This draining occurs at orifices within the ice (Fig. 2) that serve as focal points for vertically oriented axial jets with vertical motion; these orifices are called strudel, after the German word for "whirlpool" (REIMNITZ and BRUDER, 1972). Because seawater depths in the flooded areas are generally shallower than 6 m, the vertical jet encounters the bottom and may excavate craters more than 4 m deep and 20 m across (strudel scours) below the drainage points. The formerly flooded areas of fast ice generally show only very **small** amounts of fine-grained **surficial** sediment after draining is completed (REIMNITZ and BRUDER). There is a growing body of information indicating that the Sagavanirktok River contributes very little sediment at the time of river overflow.

The Holocene marine sediment **in** the study area is only 2 **to** 10 m thick (REIMNITZ et al., 1974), and delta accretion is **virtually absent** in the area (REIMNITZ et al., 1979). This Holocene sediment generally consists of fine muddy sand (BARNES, et al. , 1980); the underlying Pleistocene sediment ranges in composition from **overconsolidated** silty clay (REIMNITZ and KEMPEMA, 1980) to gravel (REIMNITZ et al., 1974). In most areas this older sediment lies within **the** range of penetration by modern strudel scours and deposits of relict and modern sediment are mixed by **the** scouring action. This mixing results in wide lateral variation and great complexity in the **surficial-** sediment types in the areas affected by strudel scour (REIMNITZ et al., 1974; BARNES et al., 1980). Because of the cut- and-fill process, high-resolution seismic records taken within the area of river overflow show an absence of coherent **subbottom** reflectors. Vibracores taken in **arctic** shallow-water-delta areas contain sedimentary structures that are interpreted as representing strudel scour fill (BARNES et al. , 1979) as discussed below. These structures, however, are too small and without horizontal continuity, to be resolvable on seismic records. Previously, REIMNITZ et al. (1974) speculated that strudel-scour relief seen near river mouths may represent several decades of strudel scour and that the scours fill in only slowly; the present studies, however, indicate otherwise.

METHODS OF STUDY

The key to the study of the **infilling** rate of strudel scours was precise navigation, which allowed us to revisit the same strudel scours in successive field seasons. This precision was provided by range/range **navigation** systems (Del Norte Trisponder and Motorola Miniranger*) aboard the 13-m research

*Any use of **trade** names and **trademarks** in this report is for descriptive purposes only and does not constitute endorsement by the U.S. Geological Survey

vessel Karluuk. Side-scan sonar and a narrow beam high-resolution fathometer ~~were~~ used to locate and survey particular strudel scours. To determine the maximum depth of a particular crater, many crossings were made in various directions, with closely spaced buoys used as reference points. ~~Once~~ the deepest point of the crater ~~was~~ located, ~~we~~ let the boat drift across with the fathometer running. This technique provided detailed cross sections.

One of the ~~two~~ strudel scours monitored ~~was~~ also marked by a metal post driven into the center by divers, by a 45-kg weight placed next to the post, and by a 35-m-long steel cable stretching from this weight to a Danforth anchor well away from the rim of the crater. The cable ~~was~~ located in successive years and led divers back to the post. The post was notched at 10-cm intervals to provide detailed observations of sediment accretion.

RESULTS

Strudel scour A

One of the strudel scours monitored is located near Egg Island Channel (A, Fig. 1), a tidal channel connecting Simpson Lagoon with the open ocean. The bathymetric map (Fig. 3) is the result of a detailed bathymetric survey of the channel on September 3, 1978, during ~~which we~~ crossed the strudel scour. Figure 3 shows the position of the strudel scour, the **trackline** crossing it, and the fathogram recorded along this track. In this fathogram, the axis of Egg Island Channel lies at a depth of 6 m, the center of the strudel scour at 5*5 m, and the surrounding lagoon floor at 2.4 m. No attempt was made, however, to determine the maximum depth of this crater **during** this first year

of record, although from past experience with strudel-scour surveys, a maximum depth of 1 m greater than shown on this chance crossing is likely.

Strudel scour A was resurveyed on August 24, 1980, with more than 20 trackline crossings; Figure 3 shows the deepest cross section recorded. The crater was still a symmetrical cone, but its maximum depth in 1980 was 4.4 m. Considering that 2 years earlier the strudel scour was more than 5.5 m deep (possibly 6.5 m), 1.5 to 2.1 m of sediment had accumulated within that period. Sediment reworking is known to occur from July through September, but may also occur during the overflow in June. Therefore the strudel scour actually trapped sediment for 8 months, at a sediment deposition rate of 15 to 25 cm per month.

Strudel scour B

A side-scan-sonar search for specific strudel scours on the Sagavanirktok delta on September 17, 1978, resulted in the selection of strudel scour B (Fig. 1) in an area generally 2.5 m deep. The base of the scour-crater was 3.5 m below the surrounding sea floor, and the crater was 16 to 25 m in diameter (Fig. 4). The side-scan sonar shows the surrounding sea floor marked by an irregular pattern of distinct curving to jagged reflectors, visible on the fathogram as 20- to 30-cm-high ledges (northeast side of strudel scour, Fig. 4). During dives along the steel grappling cable across this terrain, we found small scarps cut into firm-bedded sandy silt, which could be broken off by hand. Low terrain between these scarps was blanketed by fine sand. The upper lip of the crater itself was a 10- to 50-cm-high scarp cut into bedded sandy silt. Entering the crater from the east side and descending to the floor, we first traversed several small scarps of bedded silt, thinly draped

by soft sandy sediment, lying at the angle of repose. In the lower half of "the strudel scour was muddy sand, 20 to 70 cm thick, sloping evenly toward the center at an angle of about 30°. Although visibility inside the crater was very poor, ~~we~~ could feel the floor as a dish-shaped depression covered mainly **by** coarse fibrous organic matter, including sticks and branches. It was not difficult to drive a 3-m-long metal fencepost with a sharpened tip to about 80 Cm, but this fencepost could be driven no farther by pounding with a 1.8-kg mallet. We believe that this point represented the original bottom of the strudel scour and that the scour ~~was~~ originally 80 cm deeper than it was at the time of our survey. Ascending, ~~we~~ found the west wall to consist entirely of firm sandy silt, forming ledges 50 to 80 cm high, overhanging in places as much as 50 cm, and lacking any soft sediment cover; several ledges ~~were~~ rich in fibrous organic matter. The angularity of the firm faces of the ledges suggests erosion by undercutting and calving of firm materials. A **large** sample of organic material from the floor of the scour contained a few pebbles up to 5 cm in diameter, algal debris along with distinctly terrestrial organic material, and muddy sand.

Divers revisited the strudel scour on July 26, 1979 by following the steel cable to the pole, where the cable disappeared in very soft fill. **At** least **surificially** this fill was muddy sand and again formed a dish-shaped, rather than a **flat**, crater floor. As measured against the fencepost, 85 cm of material had accumulated since September 19, 1978 (Fig. 3), preferentially on the east side of the scour. Assuming that this sediment must have accumulated during a 10-day period in September 1978 and a 2-month period (June-July) in 1979, the sediment accumulation rate was 35 cm mo⁻¹. Divers again descended on strudel scour B on August 22, 1980. By this time major modifications had

occurred on **the sea floor**, and the strudel scour was nearly filled. We **followed** the cable to the point **where** it disappeared vertically into the sediment, extending toward the former strudel-scour floor.

The surface of the strudel-scour fill was rippled fine sand.' The top of the fencepost did not protrude because we had purposely kept it below the level **of** the surrounding terrain to avoid ice damage. The cable extending away from the crater was slack and draped across or around ledges of firm bedded sandy silt with **angular** fresh-appearing scarps as much as 50 cm **high**. **Between** ledges, the cable was deeply buried in fine muddy sand that required considerable effort to clear. Figure 5 shows a **sonograph** of the **rough** terrain adjacent to strudel scour **B**, as recorded on the date of the final inspection, **when** 2-m visibility and fresh-appearing exposures on this day allowed a closer study of the firm friable bedded sandy silt exposed in scarps. Individual **bedding** planes were highly contorted on a small scale **and** over distances of 1 to 2 m showed large-scale distortions that changed the attitude from horizontal to nearly vertical. Bedded exposures in places **were** rich in coarse fibrous organic material.

In the period between the 1979 and 1980 observations of strudel scour B, at most 4 months **of** open-water and sediment-transport conditions and **infilling** of the strudel scour had elapsed. **During** this period, 2.65 m of fill accumulated in the scour, at an **average infilling** rate of approximately 60 cm mo^{-1} .

SPACING OF STRUDEL SCOURS

REIMNITZ et al. (1974) used side-scan-sonar records to map the distribution of strudel scours in coastal areas of the Beaufort Sea. Because

of the difficulties in identifying with certainty all strudel **scours** within the seafloor areas scanned, they preferred to present only counts of strudel scours per kilometer of ship's track rather than per square kilometer of sea floor. Many additional years of shallow-water **work** in the same areas have convinced us that those original counts (maximum 25 scours km⁻¹) are much too high. Not all isolated patches of high reflectivity are strudel scours, and positive identification requires considerable fathometer-survey time. Therefore, we used the best available aerial photographs for counting the number of strudels in the previous winter's ice canopy of the study area. Figure 6 shows the **Sagavanirktok** delta on June 26, 1970, **when** one of us also made ground and aerial observations in the area. All the river water had drained off the ice 2 to 3 weeks earlier, and only the outer fringes of the formerly inundated ice remained intact. In order to count the number of strudel, we drew circles to mark areas with distinct, apparently coherent channel patterns on the ice. **Surficial drainage** channels feeding a particular strudel do not seem to extend farther than about 100 m; thus, even where the exact spot of drainage through the ice cannot be detected in this photograph, a strudel lies somewhere within each circle. These circles mark major strudel, likely to result in substantial bottom excavations. In addition, however, many more minor strudels are present. In the ice areas so studied, there **was** an average of 2.5 major strudel per square kilometer.

DISCUSSION

The **two** strudel scours monitored in this study, situated in strongly **con-**trasting environments, represent highly efficient natural sediment traps. Strudel scour A was sheltered from all sides by barrier islands or by areas

shallower than 2 m. Westerly storms, resulting in high sea levels, could provide for longer fetch than the predomimnt northeasterly wind and, probably, for bottom **reworking** at the site. Such storms did not occur during the monitoring period. **Thus**, sediment transport in the area **was** associated mainly with currents flowing through the nearby tidal channel. The flow is either **lagoonward** or **seaward**, and **we** have measured surface current velocities unrelated to tides of about 100 cm s^{-1} . During a period of several months (May-November, 1979), a current-meter array deployed in the axis of the tidal channel **was** buried by sediment to about 2 m above the original channel **floor** (Brian Matthews, oral communication, 1979). The **lower** accumulation **rates** in **the** strudel scour, not subject to scouring by horizontal currents, are unexplained.

Strudel scour B is exposed to a fetch of 20 km from the northeast, the **dominant** wind direction. Much of the area between strudel scour B and the windward barrier islands has a water depth of 6 to 7 m; furthermore, there is no flow obstacle to wind-driven currents that develop here with easterly winds (Barnes, et al., 1977). The more exposed position of this site relative to that of strudel scour A probably accounts for the more rapid **infilling** of strudel scour B.

A current meter moored for most of one summer at a depth of 5.5 m several kilometers north of strudel scour B, recorded mainly westward currents, averaging 15 cm s^{-1} but peaking at 53 cm s^{-1} (Barnes et al., 1977). No major storms occurred during those 52 days of recording, although peak velocities were high enough to move coarse sand easily. Also, numerous bottom drifters released in Stefansson Sound washed ashore far **westward** of their release points (our own unpublished data, 1979); thus, net water movement near the

bottom clearly is **westward**. The magnitude of **westward** bedload transport at another site on the Sagavanirktok delta, with nearly identical setting, 2.5-m water depth and 13-m s^{-1} easterly winds, was observed during a diving investigation in 1976 (Reimnitz and **Toimil**, 1977). Near-bottom currents of 25 to 50 cm s^{-1} moved fine sand, kelp, willow leaves, grassy material, and twigs in 1- to 2-m-wide current-parallel streaks. **At** the time of the investigation, divers observed drag marks formed by pebbles with attached kelp moving along the bottom.

These data and the following additional observations on strudel scour B suggest that its fill represents largely **bedload** transport: (1) the fathogram and diving observations show an asymmetric cross section, with the deepest point closer to the southwest wall and foreset beds of fine sand draped at the angle of repose from the northeast lip of the crater toward the center; (2) the fill consists largely of sand-size material, coarse fibrous organic matter, and a few pebbles, whereas summer-suspended matter is largely silt and clay size (DRAKE, 1977); the fibrous organic matter is rarely seen on the sea surface but is abundant on the bottom, and (3) observed at **two** intermediate stages of **infilling**, the strudel scour was conical, whereas **infilling** from suspension load should have resulted in nearly horizontal bedding planes and a flat floor.

Another strong argument in support of our contention that the **strudel**-scour fill represents mainly bedload transport is provided by the data from seven suspended-sediment traps deployed nearby in 1980. These traps, which had orifices of 30.5 cm at a height of 30.5 cm above the bottom, **were** placed in a 2-km^2 area 4 km east of our study area, in water 3.5 m deep from mid-July 1980 to about the end of the year. The traps were deployed to monitor

sedimentation around an artificial drilling island during construction. During the 5 to 6 months of deployment, an average of 13.5 cm of sediment with a median diameter of 0.1 mm accreted in the traps (NORTHERN TECHNICAL SERVICES, 1981). This accumulation represents approximately one **seasonal** sedimentation cycle plus artificial contributions from gravel island construction. Yet the accumulation rate in the suspended sediment traps was an order of magnitude lower than that in strudel scour **B**.

During the 1978 and 1979 diving inspections, ~~we~~ found coarse fibrous organic matter and a few pebbles near the bottom of the crater; higher above these organic deposits, sandy materials rested along the sides. During the final inspection dive, when infilling was complete, the **surficial** deposits of the strudel scour consisted of clean sand. This vertical sequence of materials probably is typical of all strudel scour fill in this area. The internal sedimentary structures of strudel-scour fill **should** reveal the mechanism of lateral infilling, and sediment textures should display better sorting in the uppermost section of the fill which reflects the final stages of **infilling**.

In support of the above speculation on the **nature** of strudel scour fill, Figure 7 shows a 1.5-m-long vibracore collected 2,000 m southwest of strudel scour B. BARNES et al. (1979) reported that this core is typical of a series of 12 cores taken in shallow waters on four arctic river deltas. Only features relevant to strudel scouring of the seabed, and the strudel-scour **infilling** are mentioned here. The core shows evidence of several erosional episodes: rip-up material and **mudballs**, a thick unit of coarse fibrous organic matter on an erosional surface, and a thick unit of steeply dipping bedded sand on an erosional surface; the core also contains several **ripple-bedded** sand units. The orientation of the coring device was recorded, and the

beds dip westerly. This core may record several scour-and-fill events. Most important, very little sediment suggesting settling from suspension is seen in this and the other 11 shallow-delta cores of BARNES et al. (1979); the bulk of the material probably was supplied as bedload, and deposited in scour depressions. The structures observed by divers in 30- to 50-cm-high ledges on the sea floor surrounding strudel scour B would also agree with the concept of erosion, bedload transport, and deposition, as described above.

Assuming that the fill of strudel scour B indeed represents bedload and that the crater is an efficient trap, we can use the rate of infilling to calculate the rate of bedload transport past the site. A north-south oriented cross section of the crater measured 20 m wide at the sea floor. The crater volume, calculated from the first-measured profiles and assuming a conical shape, was 360 m³. In reality, the original shape was probably more cylindrical than conical, judging from the nearly vertical west wall. Thus, the crater collected 180 m³ of bedload in a year. Divided by the 20-m width of the trap, the bedload transport rate past a 1-m seafloor segment is 9 m³yr⁻¹. During the final stages of infilling, the well-sorted sands collected to form a cap for the fill, and the former crater was no longer an efficient trap for bedload. We believe that the final stages of infilling occurred during particularly windy fall days of 1979, not during the summer of 1980, when we last looked at strudel scour B. Thus, because of the decreasing efficiency and early completion, and the conical shape conservatively used in the calculations, the actual bedload transport rate is certainly higher than the calculated rate. Because weather records for the two seasons of bedload trapping show very little winds from the west and strongest winds from the east, the calculated bedload-transport rate is probably nearly equal to the net westward transport rate.

The following considerations will demonstrate the significance of the above measurements. The transport rate of $9 \text{ m}^3 \text{ yr}^{-1} \text{ m}^{-1}$ past strudel scour B, which probably applies to a wide area, suggests very high rates of sediment movement on the shelf. From the shore to the 3-m isobath the delta front is a gently sloping surface, about 4.5 km wide in a section oriented at a right angle to the westward transport. Strudel scour B lies near the outer edge of this platform, where transport rates probably are lower than at shallower depths shoreward. If the measured transport rate is applied to the total width of this platform, a value of $40,500 \text{ m}^3 \text{ yr}^{-1}$ of sediment is derived, most likely a conservative estimate. NUMMEDAL (1979), on the basis of his own calculations and a summary of published data from the north shores of Alaska, estimates the transport rate along present barrier beaches at "a few tens of thousands of $\text{m}^3 \text{ yr}^{-1}$." This longshore-transport estimate nearly equals our measured bedload-transport rate over only a narrow segment of the shallow shelf. Resolution Island, an artificial island built several hundred yards from strudel scour B, contains $131,000 \text{ m}^3$ of gravel, a small volume relative to the sediment volume moved by nature. A comparison of the yearly bedload transport rate to the small amount of sediment that actually accumulated at the site since the last transgression, reveals the dynamic nature of the environment. The base of the Holocene marine sediment in the area, or the base of the modern Sagavanirktok River delta seen in seismic reflection records, lies only 2 to 3 m below the sea floor. This depth was confirmed by drilling (EVANS et al., 1980).

The high rates of bedload transport, together with the low rates of sediment accretion, attest to the dynamics of this depositional environment. The fresh ledges observed by divers and seen on side-scan sonar, and the deep burial of our grappling cable below clean sand, are further evi-

dence. These findings suggest that the abundant ice gouges seen in shallow **shelf** areas exposed to drifting ice, represent **only** a few years of ice activity. BARNES and REIMNITZ (1979) **showed** that waves and currents in one relatively ice-free season with long **fetch** can transform a heavily ice-gouged terrain into one of sediment waves extending out to 10-m water depths without leaving remnants of previously existing gouges. This bottom **reworking** probably occurred during only one or **two** storms.

Given such high transport rates under natural conditions, the effects of most dredging, drilling-mud discharge, and island-construction activity on the environment **would** seem to be insignificant. **However,** the contemplated construction of long causeways for offshore oil development, **which** probably **would** trap much of the sediment in transit (BARNES and MINKLER, 1982), **would** result in drastic changes to the environment within only a few decades.

The ongoing strudel scouring and subsequent **infilling** of **such** excavations result in characteristic structures that should serve as unmistakable criteria for the recognition of ancient high-latitude **deltaic** deposits formed in similar environments to a **water** depth of at least 5 m. The following considerations reveal just how dominant the structures resulting from such cut and fill action should be. An average of 2.5 large strudel per square kilometer **were** mapped in the ice canopy off the Sagavanirktok River. We estimate that all these drainage systems were large enough to create a typical 15-m-diameter 3-m-deep scour depression on the sea floor below. Given these values, any square kilometer of sea floor in this area would be reworked to a **subbottom** depth of at least 2 m, where the craters still have vertical **walls**, every 2,300 years; **reworking** to the full 6-m depth of strudel scouring **would** require more time. BARNES et al. (1979) noted the typical delta sequence seen

in 12 vibracores and the importance of strudel scour structures. They further noted that of three **vibracores** taken over a 50-m distance, each vibracore showed a typical delta sequence: bedded and **crossbedded** clean sand layers alternating with layers of fibrous organic matter. None of these distinct units, however, could be correlated over distances of 20 to 30 m. The vibracore taken near strudel scour B clearly indicates the futility of trying to trace individual beds even for short distances.

CONCLUSIONS

- (1) Strudel scours as much as 25 m across and 6 m deep are excavated at a rate of $2.5 \text{ km}^2\text{yr}^{-1}$ and are infilled with sediment after 2 to 3 years. At this rate the entire delta front of arctic rivers should be totally **reworked** in several thousand years and, therefore, should consist entirely of **strudel-scour** deposits.
- (2) Strudel scours trap materials supplied almost exclusively by **bedload** transport. For the first year or **two**, they are efficient natural traps and, therefore, should provide accurate bedload-transport rates.
- (3) The calculated transport rate past one strudel scour is $9 \text{ m}^3\text{yr}^{-1}\text{m}^{-1}$. This rate, applied to a 4.5-km-wide strip of shallow water with similar conditions, gives a bedload-transport rate of $40,500 \text{ m}^3\text{yr}^{-1}$, comparable to estimates of longshore transport rates along local barrier beaches.
- (4) This rapid **infilling** rate implies that the chances of seeing a strudel scour without fill and, therefore, measuring the maximum depth on any one survey is small, and further implies that all strudel scours, as well as **shallow-water** ice gouges, record only the most recent events.

- (5) The characteristic deposits and structures: steep erosional unconformities overlain by bedded sand and coarse fibrous organic matter at the angle of repose, and the absence of horizontal continuity can be used to identify ancient deposits from similar environments.
- 6) In view of the very high rates of sediment transport determined for natural conditions, the sediment input from human activities, such as dredging operations, seems insignificant. However, long causeways planned for the offshore oil development **would** act as groins and result in large-scale shoreline modifications.

ACKNOWLEDGMENTS

This study **was** funded in part by the Bureau of Land Management through interagency agreement with the National Oceanic and Atmospheric **Admini-**stration, as part of the Outer Continental Shelf Environmental Assessment Program. We thank Doug Maurer for his help in the early phases of fieldwork and diving observations on strudel scour B.

FIGURE CAPTIONS

- Figure 1. Landsat images of Prudhoe Bay area (between A and B) on June 6, 1976, showing larger rivers flowing out across the fast ice. In many years, flooded ice areas nearly merge in this area.
- Figure 2. Overflow ~~water~~ from Kuparuk River draining at a strudel situated on a crack in 2-m-thick fast ice. Overflow at this point is estimated to be 1 to 1.5 m deep, and the water below the ice is 1 to 2 m deep. Distance across center of the photograph is about 15 m.
- Figure 3. Site of strudel scour A adjacent to Egg Island Channel, in relatively sheltered locality. Inset shows fathogram across tidal channel and scour in **1978**, with 1980 profile superimposed. 1978 crossing of strudel scour A was by chance, and scour could have been deeper than actually measured.
- Figure 4. Fathogram of deepest profile of strudel scour B in **1978**, and ~~two~~ successive years. Divers found vertical walls on upper 1 m of left (~~west~~) side and estimated original scour depth by driving the stake shown .
- Figure 5. Sonograph of sea floor adjacent to strudel-scour B after complete **infilling** in 1980, showing the rough relief with fresh-appearing ledges seen by divers.

Figure 6. **Orthophoto** of Sagavanirktok delta showing remnants of fast ice on June 26, 1970. Drainage systems feeding former strudel are circled.

Figure 7. Resin peel of a vibracore taken 2,000 m from strudel scour B. Core records several scour-and-fill events. Core is oriented with right side to west (from Barnes et al., 1979).

REFERENCES

- BARNES P. W. (1982) Hazards. In: Beaufort Sea Synthesis-Sale 71, D. W. ,
NORTON, and W. M. **SACKINGER**, editors, NOAA, Office of Marine **Polution**
Assessment, Juneau, Alaska, p. 89 (in press).
- BARNES P. W. and P. W. MINKLER (1982) Sedimentation related to causeway
construction, Prudhoe Bay, Alaska. In: National Oceanic and Atmospheric
Administration, Environmental Assessment of the Alaskan Continental
Shelf: Principal Investigators Reports, Attachment A of 1981 Annual
Report, 7 pp.
- BARNES P. W., ERK **REIMNITZ**, and DAVID McDOWELL (1977) Current meter and water
level observations in Stefansson Sound, summer, 1976. In: Miscellaneous
hydrologic and geologic observations on the inner Beaufort Sea shelf,
Alaska. P. W. BARNES, ERK **REIMNITZ**, D. E. DRAKE, and L. J. **TOMIL**, U.S.
Geological Survey Open-File Report 77-477, B-1 to B-7.
- BARNES P. W. and ERK **REIMNITZ**, (1979) Ice gouge obliteration and sediment
redistribution event - 1977-1978, **Beaufort** Sea, Alaska. U.S. Geological
Survey Open-File Report 79-848, 22 pp.
- BARNES P. W., ERK **REIMNITZ**, L. J. **TOMIL**, D. M. **McDOWELL**, and D. K. **MAURER**,
(1979) Vibracores, Beaufort Sea, Alaska: Descriptions and preliminary
interpretation. U.S. Geological Survey Open-File Report 79-351, 103 pp.
- BARNES P. W., ERK **REIMNITZ**, and ROBIN ROSS (1980) Nearshore **surficial** sediment
textures--Beaufort Sea, Alaska. U.S. Geological Survey Open-File Report
80-196, 41 pp.

DRAKE D. E. (1977) Suspended matter in nearshore waters of the Beaufort Sea (1976) In: Miscellaneous hydrologic and geologic observations on the inner **Beaufort** Sea **shelf**, Alaska. P. W. BARNES, **ERK REIMNITZ**, D. E. DRAKE, and L. J. **TOIMIL**, U.S. Geological Survey Open-File Report 77-477, c-1 to **C13**.

EVANS C. D., J. J. WILSON, J. C. LaBELLE, J. L. WISE, S. **CUCCARESE**, D. TRUDGEN, R. BECKER, A. L. **COMISKEY**, J. BALDRIDE, and S. WILSON (1980) Environmental review of summer construction of gravel islands: Sag Delta No. 7 and No. 8, **Stefansson** Sound, Alaska, Arctic Environmental Information and Data Center (**AEIDC**), Prepared for **Sohio Alaska Petroleum** Company.

HUBBELL D. W., (1964) Apparatus and techniques for measuring bedload. Geological Survey Water-Supply Paper 1748, 74 pp.

MATTHEWS J. B. (1981) Observations of under-ice circulation in a shallow lagoon in the Alaskan Beaufort Sea. Ocean Management, 6, 223-234.

NORTHERN TECHNICAL SERVICES (1981) Environmental effects of **gravel island** construction. Endeavor and Resolution Islands, Beaufort Sea, Alaska, Prepared for **Sohio** Alaska Petroleum Company, Anchorage, Alaska, 62 pp.

NUMMEDAL, DAG, (1979) **Coarse-grained** sediment **dynamics--Beaufort** Sea, Alaska. **In:** Proceedings of Port and Ocean Engineering Under Arctic Conditions, **Norwegian** Institute of Technology, 845-858.

REIMNITZ, ERK and K. F. BRUDER (1972) River discharge into an ice-covered ocean and related sediment dispersal, Beaufort Sea, coast of Alaska. Geological Society of America Bulletin, **v.** 83, no. 3, 861-866.

REIMNITZ ERK, C. A. **RODEICK** and S. C. WOLF (1974) Strudel scour: A unique arctic marine geologic phenomenon. Journal of Sedimentary Petrology, v. 44, no. 2, 409-420.

- REIMNITZ, ERK, and L. J. TOIMIL (1977) Dive-site observations in the Beaufort Sea, Alaska--1976. National Oceanic and Atmospheric Administration, Environmental Assessment of the Alaskan Continental Shelf: Principal Investigators Reports, Apr. - June 1977, 2, 457-558.
- REIMNITZ ERK, K. H. DUNTON and P. W. BARNES, (1979) Anchor ice and lack of delta accretions in the Arctic--A possible link. Geological Society of America, Abstracts with Programs, v. 11, no. 7, 501.
- REIMNITZ, ERK and E. W. KEMPEMA (1980) Super sea-ice kettles in the arctic nearshore zone - Reindeer Island. In: National Oceanic and Atmospheric Administration, Environmental Assessment of the Alaskan Continental Shelf: Annual Reports of Principal Investigators for the year ending March, 1980, v. 4, 344-355.
- WALKER H. J. (1974) The Colville River and the Beaufort Sea: Some interactions. In: The Coast and Shelf of the Beaufort Sea. J. C. REED and J. E. SATER, editors, Proceedings of the Arctic Institute of North America Symposium on Beaufort Sea Coast and Shelf Research, Arlington, Virginia, Arctic Institute of North America, 513-540.



OTC 4310

Observations on the Mode and Rate of Decay of an Artificial Ice Island in the Alaskan Beaufort Sea

by Erik Reimnitz, Edward Kempema, and C. Robin Ross, U.S. Geological Survey

This paper was presented at the 14th Annual OTC in Houston, Texas, May 3-6, 1982. The material is subject to correction by the author. Permission to copy is restricted to an abstract of not more than 300 words.

ABSTRACT

In the Arctic ice is abundant and cheap, and therefore has long been considered as structural material for offshore drilling platforms. In February 1979 Exxon constructed an ice island 400 m in diameter and 10 m thick, in water 3.5 m deep, about 6 km north of Prudhoe Bay, Alaska. The purpose of the experiment was to learn whether such an island could survive one summer and then serve as a platform for an extended drilling period the following winter. Our studies of the decay of this island are based on: a) surface observation and photography, b) diving observations and bottom photos, c) fathometer, subbottom profiler and side-scan sonar surveys, and d) spot measurements of water salinity, temperature, and turbidity around the island.

Thermal erosion, promoted by turbulent heat transfer from wave action and a relatively warm surface water layer surrounding the island, resulted in a 3- to 5-m-deep notch at sea level, frequent calving, and a cantilevered, vertical scarp above sea level around the island. The winds, waves, and surface currents that transport warm river water past the island are predominantly from the east. Therefore, thermal erosion and calving were most rapid on the east side; they had truncated the island to the original center point by late August. By early September, the last remnants of the island floated away. The submerged part of the island, below the sea-level notch, consisted of an extensive pedestal reaching as much as 15 m beyond the island and feathering out to 10 cm thick at the lip. The outer 5 m of this pedestal was elevated above the flat sea floor, forming a gap up to 25 cm wide that exposed the smooth base of the island to divers. Average island shore erosion, effected largely by calving, ranged from 2.5- to 5-m/day. The pedestal retreated across the sea floor at the same rapid rate, but melting, rather than calving, was probably the major cause of erosion. Hydraulic processes did not have time to develop cut-and-fill structures in the sea floor. In short, the test showed that unprotected ice islands in shallow, warm coastal waters have no chance of survival through the summer.

INTRODUCTION

Ice interacts with the marine environment in many different ways, and through these interactions becomes an important geologic agent. The U.S. Geological Survey has conducted research on ice-related processes for many years. Recent petroleum developments in northern Canada and Alaska have focused attention on ice in the marine environment and on the effects of the ice on shores and the shelf surface. During the winter of 1978-1979, a circular ice island with a diameter of 400 m was built in the shallow waters of Stefansson Sound, about 6 km north of Prudhoe Bay, Alaska (Fig. 1). This large, firmly grounded mass of ice of known age, size, and shape provided a unique opportunity to study the effects of summer conditions until the island was destroyed by natural processes before winter.

BACKGROUND INFORMATION

In the Arctic ice is abundant and cheap and therefore has long been considered as a potential structural material for offshore drilling platforms.^{1,2,3,4} Several field experiments with ice drilling islands have been conducted in Alaskan waters. In 1969, attempts were made to firmly anchor a grounded, natural ice island by ballasting it with an added surface layer of ice. This island was located at about 25-m water depth, where it was fully exposed to drifting pack ice. For reasons not entirely clear, this island broke up during the studies.⁶ In early 1977 an artificial ice island was built by Union Oil Co. at 3-m water depth in Harrison Bay. An exploratory well was drilled from this island before the ice decayed in July, 1977. Being located within the smooth, immobile fast ice of Harrison Bay, this island was relatively safe from the effects of shifting ice, but the nearby discharge of warm Colville River water, which resulted in early ice-free conditions in the area,⁷ was largely responsible for the fast decay of this artificial ice island.

In February 1979, Exxon began construction of an experimental ice island in Stefansson Sound, about 6 kilometers north of Prudhoe Bay (Fig. 1).

The purpose was to learn whether this test structure could survive one summer and then serve as a platform for an extended drilling season during the following winter.

Studies of icebergs show that **their** deterioration is basically due to melting.⁸ The ice masses receive energy by radiation, convection, and conduction from the air, water, and sun. According to Kollmeyer,⁹ turbulent heat transfer is of prime importance for ice decay. Thus, icebergs have extended lives as long as they remain protected by sea ice, which reduces wave turbulence. Wave turbulence prevents a static, **cold-water boundary** layer from forming around the iceberg.⁸ The pronounced notches at sea level that are usually seen around drifting ice, attest to the effectiveness of wave turbulence in reducing the size of ice. There is, however, an important difference between the processes effective on drifting ice and those effective on grounded ice. A grounded ice mass is no longer moving with the water, and therefore it encounters relatively higher flow velocities to transport away cold melt water. Because of these considerations, a brief description of the marine environment at the ice island site is in order.

The water depth at the Exxon ice island site is nearly 3.5 m. The bottom, which is essentially flat, consists of very fine, muddy sand. During winter the site lies within the zone of floating fast ice. The floating ice moves only a few meters, and it reaches a thickness of up to 2 m at the end of the winter. During summer, the area is protected from pack-ice incursions by a chain of barrier islands. Beginning in late May or early June, the Sagavanirktok River (Fig. 1) discharges relatively warm water only a few kilometers east of the site. With the dominant easterly winds, this warm water flows westward past the ice island. In 1976, for a period of 52 days starting in late July, oceanographic sensors were deployed 1 m off the bottom near the ice island area. These sensors provided information about salinity, **temperature**, tides, and currents for the open-water season.¹⁰ The astronomical tidal range is only about 15 cm, whereas sea-level fluctuations from changing winds and barometric pressures normally are several times larger. The recorded average near-bottom current velocity was 15 cm/sec, with one peak of 53 cm/sec, sufficient to erode and transport coarse sand. Our extensive boat and diving experience in the area indicates that surface current velocities commonly are several times higher than bottom velocities. The bottom-water temperature during the period of record ranged from -0.9 to **7.5°C**; the water at the surface was generally several degrees warmer. The salinity ranged from 12.8 to 30.6 parts per thousand. In July 1972, regional surveys in the area showed a freshwater plume with salinity of about 2 parts per thousand extending from the Sagavanirktok River past the site. Further studies by Woodward-Clyde Consultants¹¹ show that the water mass in Prudhoe Bay and vicinity is largely stratified, especially under easterly wind conditions. The **upper layer** is primarily Sagavanirktok River water, being relatively warm (i.e. **6°-9°C**) and relatively fresh (i.e. 15 to 20 ppt). The lower layer is water of almost totally oceanic origin, being colder, (**1°-4°C**), and more saline (30-33 ppt).

Wave activity begins in late June at the island site; the fetch to the east increases to its maximum by late July. Because of the **restricted** fetch and the shallow water, we have never observed waves higher than 1 m in the area.

THE ICE ISLAND

A single, large, rotating sprinkler system fed by seawater pumps was used to construct the circular, dome-shaped ice island (Fig. 2). In the initial stages, the thin fast ice apparently was strengthened by surface flooding, with rotating augers used as Archimedes screws to lift water to the ice surface. But the spraying process **results** in considerably more rapid freezing of water.⁶ Because the sprayed water was free to spread out onto the surrounding floating sheet of ice, the **accre-**ting ice assumed a dome shape. Surface runoff toward the perimeter consisted of brine from salt excluded in the freezing process. Beyond the perimeter, the brine presumably drained through the surrounding floating fast ice. Pumping was continued until the island had an elevation of about 7 m at the center and was firmly grounded on the sea floor. The total ice thickness ranged from 10 m in the middle of the island to 6 or 7 m near the fringes". The diameter of the island was nearly 400 m.

METHODS OF STUDY

Observations and data collected around the ice island during the summer of 1979 consist of:

- a) aerial and shipboard observations and photography of the island's decay; b) diving observations and underwater photography of the ice/bottom contact; c) fathometer, sub-bottom profiler, and side-scan sonar surveys around the island; and d) spot measurements of water salinity, temperature, and light **transmissivity** around the island.

RESULTS

Surface observations.- Our first observations of the island were made in the middle of July. At that time the island was circular (Fig. 1) and slightly dome-shaped. surface drainage gullies, shear cliffs at the water's edge, active calving, and scattered ice drifting in the wake of the island were evidence that the decay was in full progress. Continued calving, resulting from lack of hydrostatic pressure on unsupported faces, was enhanced by deep erosional notches at sea level that were cut horizontally into cliffs within several hours after calving (Fig. 4). The dominant northeasterly winds and westward currents carrying relatively warm, fresh river water on the surface resulted in the most rapid erosion on the island's "weatherside". Thus the island soon assumed an asymmetric shape, as shown in Figure 5 in which the location of the pivot point of the formerly central sprayer system is near the eastern shore. To reduce undercutting and calving, a large tarpaulin, weighted at the base by a chain, had been draped over a portion of the island's perimeter. This tarp was carried away with calved ice by late July. "By the first week in September, the ice island had been reduced so much that it was hardly recognizable. On September 10th, long before the major fall storms set in, the last remnants of the island had floated away.

Diving observations. - Diving observations were made around the island on August 16, under light north-westerly winds and weak southeasterly currents. During the several days preceding the dive, the wind had been from the northeast and considerably stronger. Thus, the current flow would have been westward and relatively swift for several days before the dive. Our diving traverse partially **circumdived** the island in a counterclockwise direction, starting from a point on the southeast side of the island and ending on the west side. An idealized sketch of the underwater shape of the ice island is shown in Figure 6. A sea-level notch characteristically extended from 3 to 5 meters or more underneath the ice cliff and was absent only in a few places where calving had recently taken place. Underneath this overhang, the water visibility was blurred on account of the mixing of melt and sea water having different indexes of refraction. From the sub-aerial cliffs or from the crotch of the sea-level notch there was a gentle seaward-sloping ice face. This ice surface was concave upward and slightly undulating; it extended from 5 to 15 meters or more beyond the subaerial ice cliffs. This wide submarine base of the island will be referred to as the 'ice pedestal'. The ice pedestal typically feathered out to a sharp edge (Fig. 7), where no recent upward calving occurred, or it terminated in a small **scarp** 10 to 30 cm high. The outer edge of the pedestal had an irregular, crenelated configuration, forming 3- to 4-m embayments that exposed the sandy substrate. The pedestal also contained a few isolated holes or 'windows' in ice 60 to 80 cm thick that extended down to the sea floor (Fig. 8). Much of the bottom diving traverse paralleled the very edge of the pedestal. Along most of this edge the base of the pedestal was slightly raised, forming a basal gap at the sea floor large enough to permit a diver to slide his hand between the pedestal and the sea floor. This gap varied in height from 3 to 25 cm and extended underneath the ice to at least the range of visibility (2-3 m). Even within perforations 4 m from the tip of the pedestal, the basal gap could be seen (Fig. 8), and therefore it must have extended at least 5 m underneath the ice island. Wherever the base of the ice could be seen through the gap, the face was **smooth** and parallel to the horizontal sea floor. At one location, a thin isolated slab of ice about 1 m in diameter was hugging the bottom a short distance away from the margin of the pedestal. The slab rose to the sea surface when the diver disturbed it.

The sandy sea floor adjacent to the perimeter of the ice pedestal on the east and west sides of the ice island was flat with small ripples. This flat bottom was seen to extend underneath the ice without any noticeable change in ripple pattern. Along the north side of the island, facing the very weak current of that day, small scour depressions had formed, and kelp (*Laminaria*), dead isopods, and fine sand were piled against the pedestal. Although the surface of the pedestal in most areas was essentially clean, on the north side a sediment cover up to 4 mm thick was seen in subtle depressions. Also, several cylindrical holes in the pedestal had filled with sediment, and erosion of the pedestal containing such filled holes resulted in sediment mounds up to 40 cm high--remnants of sediment filling. When we probed the sea floor

along much of the pedestal, we found no evidence of ice-bonding of sediment.

Geophysical Surveys. - Fathometer and side-scan sonar surveys were made on July 27, 1979, in a radial pattern around the island, approaching to within 15 m of the cliffs and extending several hundred meters offshore. The records show an essentially featureless bottom. In addition to this survey, several fathometer/subbottom profiler (7kHz) survey traverses were run over the ice pedestal surrounding the ice island on August 16, 1979. These traverses were run on straight courses tangential to the island, bringing the **starboard** side of the vessel with the transducer as close to the island as possible. The record of several of these tangential traverses, shown in Figure 9, **reveals** the concave upward surface of the ice pedestal. Where the vessel passed over the ice pedestal, a subbottom reflector occurring 1.5 m below the sea floor is lost. The sub-bottom reflector represents the base of Holocene marine sediments. Thus the ice, even where only 20 cm thick, is opaque to seismic signals at a frequency of 7 kHz. A side-scan sonar and fathometer survey run across the former ice-island site by P.W. Barnes of the U.S.G.S. on September 18, 1979, revealed only remnants of the plumbing system that had been used during the construction phase.

Hydrographic Measurements. - A sketch outline of the island and the hydrographic stations taken July 27 is presented in Figure 10. At the time of the measurements, **light** winds were blowing from the northeast. Measurements were made at the surface and near the bottom. The values of salinity, transmissivity, and temperature (Fig. 10) reflect the decay of the island. The island serves as a heat sink, and a west-northwest-trending wake is characterized by higher salinity, lower light transmissivity, and lower temperature than the water on the updrift side. The lower light transmissivity readings in the wake may be largely the result of the mixing of waters having different indices of refraction, as apparently no sediment is being added to the water by the ice or by bottom scour from currents. The higher salinity readings in the wake are evidence that the average salinity of the ice island is several ppt higher than that of the 15.5 ppt salinity water attacking the island from the east. The water **column was not as well** stratified on July 27 as observed on other occasions in the area.

DISCUSSION AND CONCLUSIONS

Our studies of the decay of the ice island show that the island's subaerial part was eroded mainly by cracking and calving. The melting of the breakup products increased after their immersion in seawater, while they were drifting away from the site. On the other hand, the underwater surfaces and profile show that melting is the dominant process of submarine erosion. Melting rates were highest on the east side, the side exposed to the dominant waves from the east and to the influx of warm water carried by dominant westward-flowing currents. The vertical profile reflected the combined effects of higher water temperature, higher flow velocities, and greater wave turbulence near the sea surface, as compared to the quieter

and cooler bottom waters. These factors resulted in the deep notch at sea level and the extensive pedestal feathering out to a thin edge on the bottom. We assume that the average vertical profile of the ice island was in equilibrium with the environmental parameters affecting the profile. Once the typical mushroom shape with a very wide pedestal was established, the subaerial parts retreated at the same rate as the submerged parts. Given 200 m as the original radius, June 20, 1979 as the beginning of lateral decay, and September 10, 1979 as the last day of the island, the average rate of peripheral erosion would be about 2.5 m per day. However, erosion was not equal at all points around the periphery of the island. The east side of the island, exposed to the dominant waves and currents, eroded much more rapidly than the relatively protected west side, at times reaching an estimated erosion rate of 5 m per day. The erosion rate could also vary quite a bit from the average on any given day. During periods of calm weather a protective layer of cold water could form around the island, protecting the ice from melting. The lack of waves during a calm period would result in less undercutting of the subaerial portion of the island and in less erosion of the surface of the island. Conversely, when wave heights and current velocities increased, a steady stream of relatively warm river water would be washed over the ice pedestal, and the waves would rapidly cut a sea level notch, resulting in increased calving and very rapid erosion on the exposed, weather side of the island.

The extent to which the vertical profile reflects differences in resistance to erosion is unknown. The methods used for constructing the island--i.e., adding surficial layers of ice onto a thin sheet of naturally grown ice--results in a stratified ice mass. Fitch and Jones⁶ pointed out that a major disadvantage of the spray-freezing method is that the artificial ice it produces may be "fluffy." The bottom-most, natural layer of the ice pedestal, still containing the initial auger-produced cylindrical holes, may have been the most resistant to melting. There apparently was no difference in ice texture and melting resistance between naturally grown ice, presumably about 1 m thick at beginning of construction, and the artificially grown ice above. No nickpoint was observed in the slope of the ice pedestal corresponding to a boundary between ice types. For these reasons, we feel that physical differences between ice types had little effect on the shape of the vertical profile.

Flow intensification around stationary ice commonly produces bedforms of cut and fill adjacent to and below the ice.^{12,13,14} But neither the geophysical surveys nor our diving investigation revealed major bedforms related to the island. Instead, regular, small-scale-ripple patterns on flat bottom extended without obvious changes for a distance of at least 2 m beneath the ice pedestal. Only the northern side, exposed to weak currents and small waves during the time of direct bottom observations, had small amounts of sand and kelp piled against the pedestal. The stronger northeasterly winds of the two previous days probably resulted in similar or larger piles against the northwest side, which was exposed to

the weather at that time. In our diving traverse skirting the edge of the ice pedestal, we could see outward across the sea floor only 3 m at most. Because of the rapid ice erosion rate, any bedforms or accumulations from the stronger wave and current action of the previous day would have gone unnoticed by us. Small-scale bedforms of summer scour and fill apparently are in dynamic equilibrium with rapidly changing flow conditions at the edge of the pedestal. Thus, the pedestal retreated across flat sea floor on a calm day, while any bedforms of previous turbulent flow conditions were left behind as relict features away from the pedestal.

The rather uniform space along the lip of the pedestal between the smooth ice island base and the flat, rippled sand bottom was obviously not a result of ice- or sediment-erosion by currents. This gap was probably due to plastic deformation of the thin ice at the edges of the pedestal caused by the buoyancy forces of the ice. As such, this gap probably did not extend towards the island center past the point where the ice pedestal was 1 m thick, and the center of the island remained firmly grounded.

The results of this investigation cannot be applied directly to naturally occurring masses of grounded ice. Most sea ice in the Beaufort Sea has irregular shapes, and at any given time a mass of such ice has a small base relative to the area at sea level. Also, most naturally occurring sea ice is unstable, and so calving commonly results in at least slight rotations of the ice. Grounded ice commonly has irregular, steeply sloping sides near the bottom that converge with the sea floor at angles that decrease toward the very "keel," so that the actual bottom contact commonly cannot be reached by divers.^{12,13} Unless deeply buried, most grounded ice is unstable and will change attitude during the course of several melting days. For these reasons, naturally occurring grounded ice rarely remains long enough to assume an underwater profile in equilibrium with the average characteristics of the water mass.

There may be ice islands or ice masses that are exceptions to the above generalizations. Large natural ice islands in the Arctic Ocean are tabular, presumably have a relatively flat base, and conceivably could remain in a stable orientation for extended periods, if they were grounded firmly. Two firmly grounded, relatively small ice-island fragments in MacKenzie Bay were studied in some detail after they had survived through the last days of a severe fall storm and most of the following winter.¹⁵ Soundings showed one of these to have a wide bulge, similar to that of the artificial ice island, somewhat below mid-depth but not hugging the sea floor. Also, divers described a 2- to 3-m protuberance ("shovel") near the bottom. This shovel was separated from the bottom by an unspecified distance, but this gap below the ice base conformed to what appeared to be the sloping flank of a ridge pushed up by the ice, and the gap could have formed simply by subsequent ice movement away from that ridge. Also the shovel was more massive and blunt than the ice pedestal, making it unlikely that plastic deformation had been the mechanism causing the gap. The underwater shape of

a grounded ice-island fragment off Prudhoe Bay was investigated by Breslau and Trammell⁵ in April 1969. The lateral sounding techniques they employed were inadequate to show precisely the relationship between the ice and the sea floor. A pedestal similar to the one on the artificial ice island we studied apparently had not formed there.

Our studies showed that an unprotected artificial ice island in the relatively warm coastal waters is unsuitable as a longterm drilling platform. The chances of such an ice island surviving a summer probably would be much higher if the island were placed in the cooler waters seaward of barrier islands, especially in a year with much ice and no fetch for waves and currents.

ACKNOWLEDGMENTS

This study was supported jointly by the U.S. Geological Survey and the Bureau of Land Management through interagency agreement with the National Oceanic and Atmospheric Administration under a multiyear program responding to needs of petroleum development of the Alaska continental shelf. The program is managed by the Outer Continental Shelf Environmental Assessment Program (OCSEAP).

REFERENCES

1. McKay, A.R., 1970, Man-made ice structures of Arctic marine use: **I.A.H.R. Symp.**, Ice and Its Action on Hydraulic Structures, Reykjavik, Sept. 7-10, 1970.
2. Behlke, C.E., and McKay, A.R., 1969, Artificial sea ice structures for Alaskan ports: **A.S.C.E. Ocean Eng. Conf.**, Miami, December 10-12, 1969.
3. Kingery, W.E., cd., 1963, Ice and Snow, Properties, Processes and Applications: The MIT Press, Cambridge.
4. Peyton, H.R., Johnson, P.R., and Behlke, C.E., 1967, Saline conversion and ice structures from artificially grown sea ice: U. of Alaska Arctic Environmental Eng. Lab. and Inst. of Water Resources Research Dept. No. 4, September 1967.

5. Breslau, L.R., James, J.E., and Trammell, M.D., 1970, The underwater shape of a grounded ice island off Prudhoe Bay: in Preprints of 1970 Offshore Technology Conference, Part II, p. 753-766.
6. Fitch, J.L., and Jones, L.G., 1974, Artificial ice islands could cut Arctic costs: The Oil and Gas Journal, November 11, 1974, p. 173-181.
7. Reimnitz, Erk, and Bruder, K.F., 1972, River discharge into an ice-covered ocean and related sediment dispersal, Beaufort Sea, coast of Alaska: Geological Society of America Bulletin, v. 83, no. 3, p. 861-866.
8. Robe, R.Q., 1980, Iceberg drift and deterioration, in S.E. Colbeck, cd., Dynamics of Snow and Ice Masses, Academic Press, New York, N.Y., p. 211-259.
9. Kollmeyer, R.C., 1966, U.S. Coast Guard Oceanographic Report #n, **CG373-11**, p. 41-52.
10. Barnes, P.W., Reimnitz, Erk, Drake, D.E., and Toimil, L.J., 1977, Miscellaneous hydrologic and geologic observations on the inner Beaufort Sea shelf, Alaska: U.S. Geological Survey Open-File Report 77-477.
11. Woodward-Clyde Consultants, 1981, Waterflood monitoring program status report, 31 August, 1981.
12. Reimnitz, Erk, Barnes, P.W., Forgatsch, T.C., and Rodeick, C.A., 1972, Influence of grounding ice on the Arctic shelf of Alaska: Marine Geology, v. 13, p. 323-334.
13. Reimnitz, Erk, and Barnes, P.W., 1974, Sea ice as a geologic agent on the Beaufort Sea shelf of Alaska, in Reed, J.C. and Sater, J.E., eds., **The Coast and Shelf of the Beaufort Sea**. Proceedings of the Arctic Institute of North America Symposium on Beaufort Sea Coast and Shelf Research, Arlington, Virginia, p. 301-353.
14. Reimnitz, Erk, and Kempema, E.W., 1982, Dynamic ice-wallow relief of northern Alaska's nearshore: Journal of Sedimentary Petrology (in press).
15. Kovacs, A., and Mellor, M., 1971, Sea ice pressure ridges and ice islands: CREARE Inc., Science and Technology, Technical Note no. 122, August 1971.

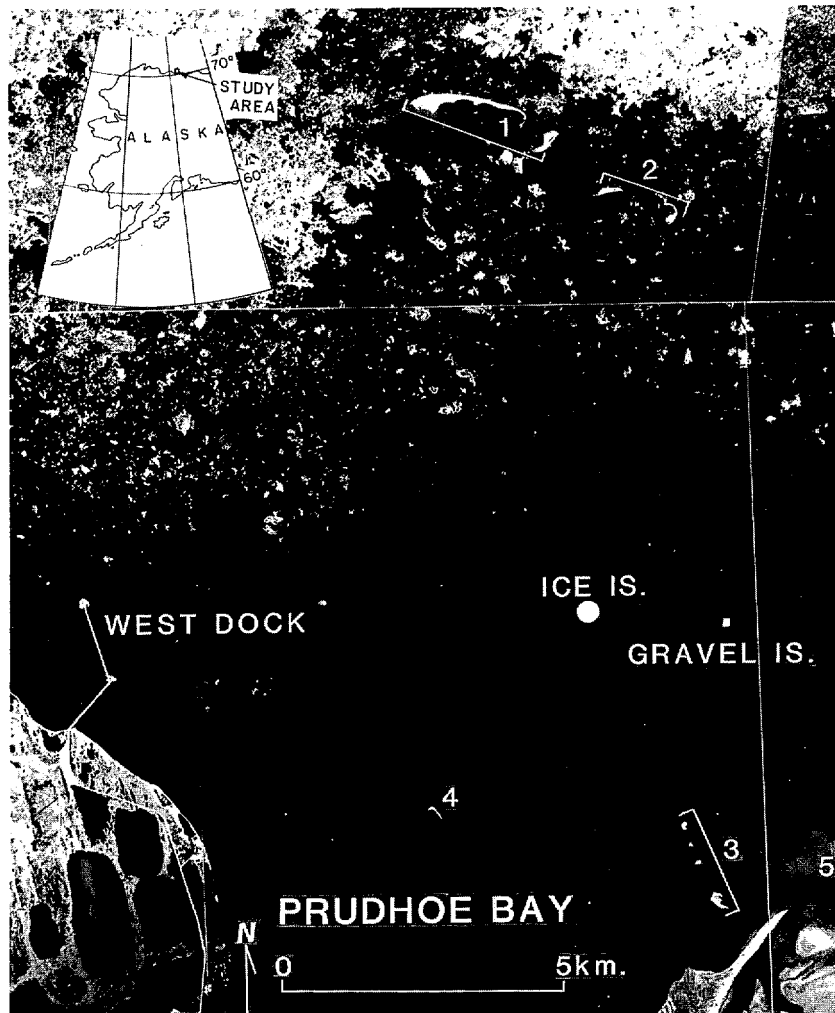


Fig. 1 — Unretouched mid-July U-2 photograph of ice island and surrounding islands: Reindeer (1), Argo (2), Niakuk (3), Gull (4), and the Sagavanirktok River (5)

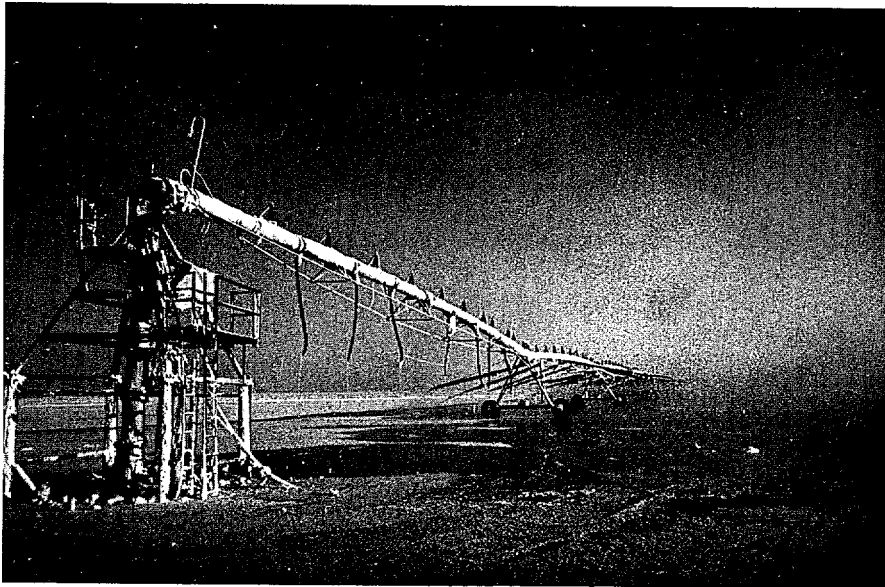


Fig. 2 — View of center-pivot sprinkler system during construction of the island in March

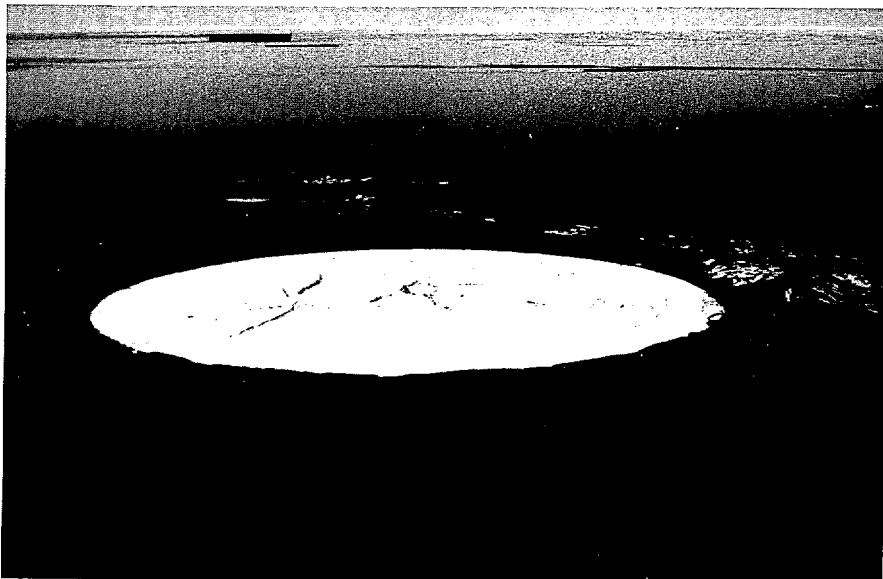


Fig. 3 — Ice island on 7-20, with the pivot point marking the center. Surface gullies, scalloped edges and a wake of calved ice debris indicate that erosion is in full progress.

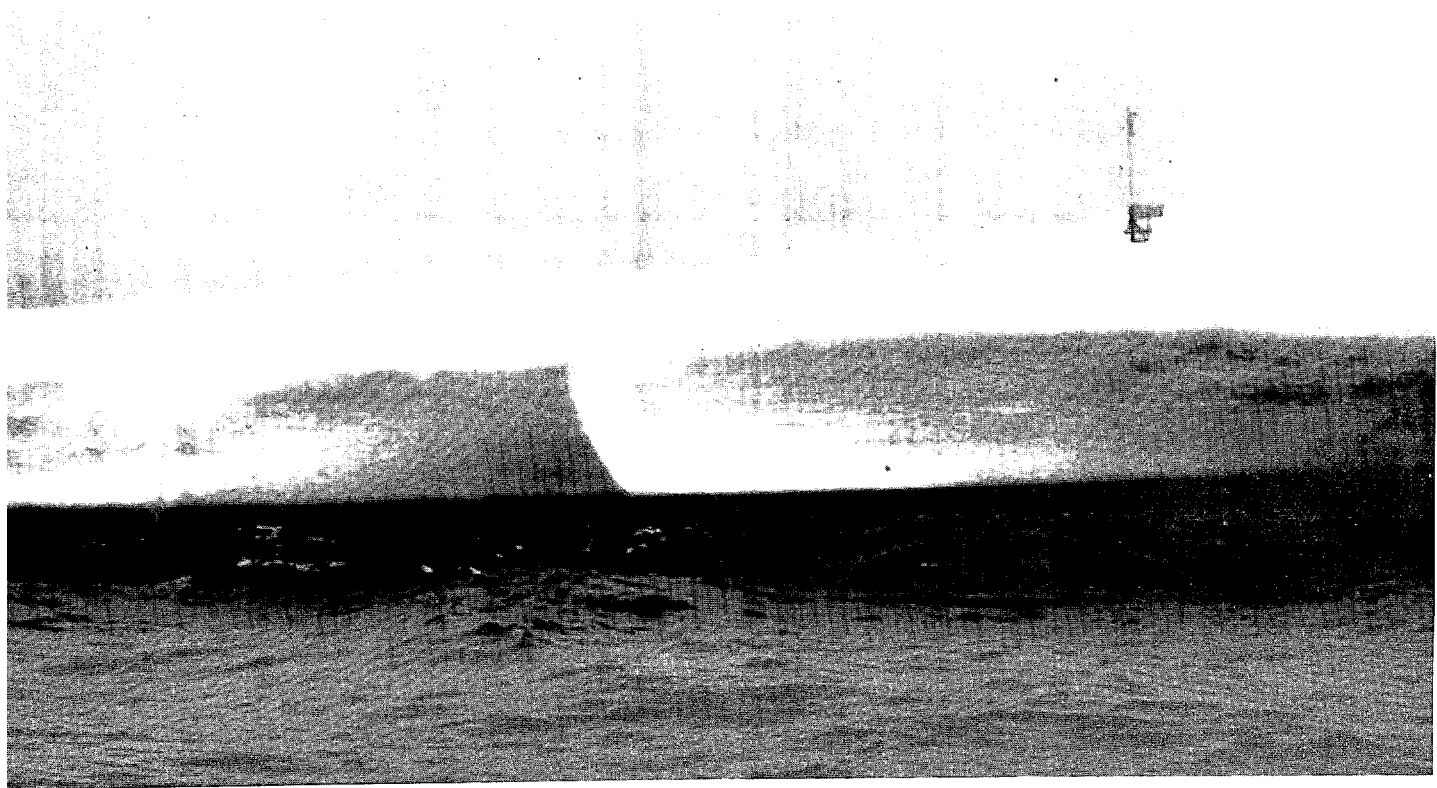


Fig. 4 — Vertical scarp of ice island, where recent calving occurred. A new horizontal sea-level notch has already been cut, setting the stage for the next calving.

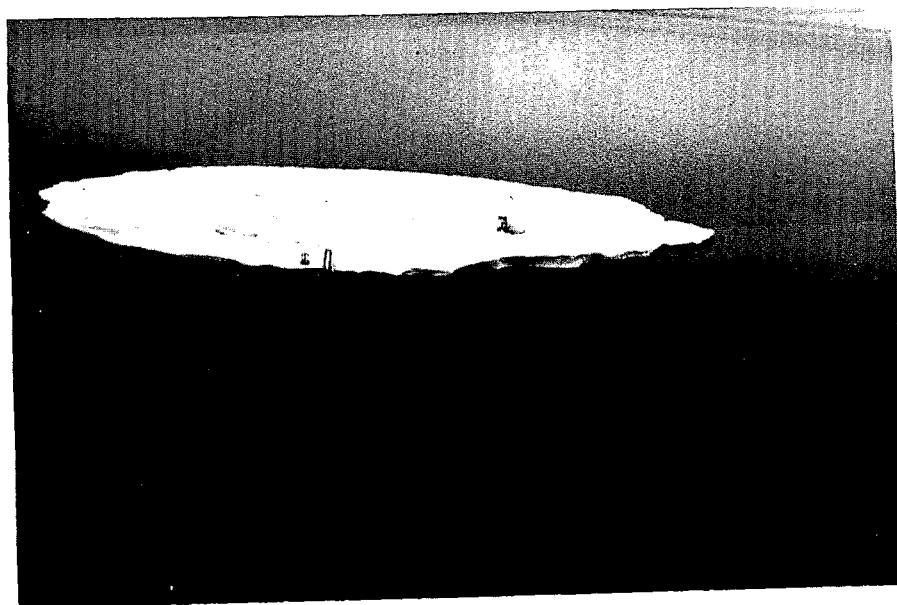


Fig. 5 — Aerial view of the artificial ice island on 8-22. Note the asymmetry of the island, with the original center pivot point (right center) near the windward shore.

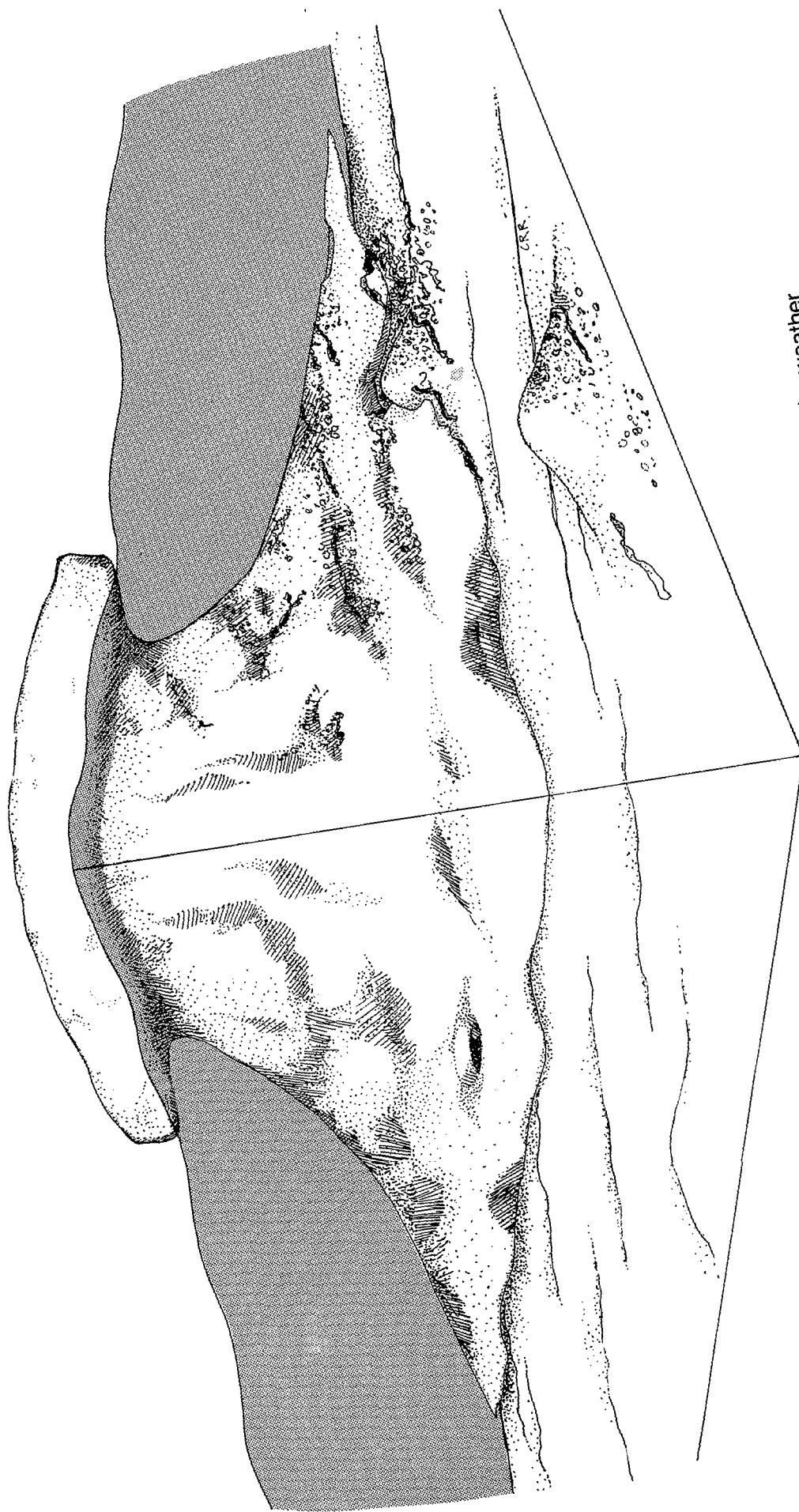


Fig. 6 — Cartoon of ice island, with accumulations of kelp and sediment on the weather side, and an auger hole (see Fig. 8) left of center in the pedestal.



Fig. 7 — Underwater photograph of the feathered edge of ice pedestal, slightly raised above the flat sea floor. An Arctic cod is hiding below the lip of the pedestal.

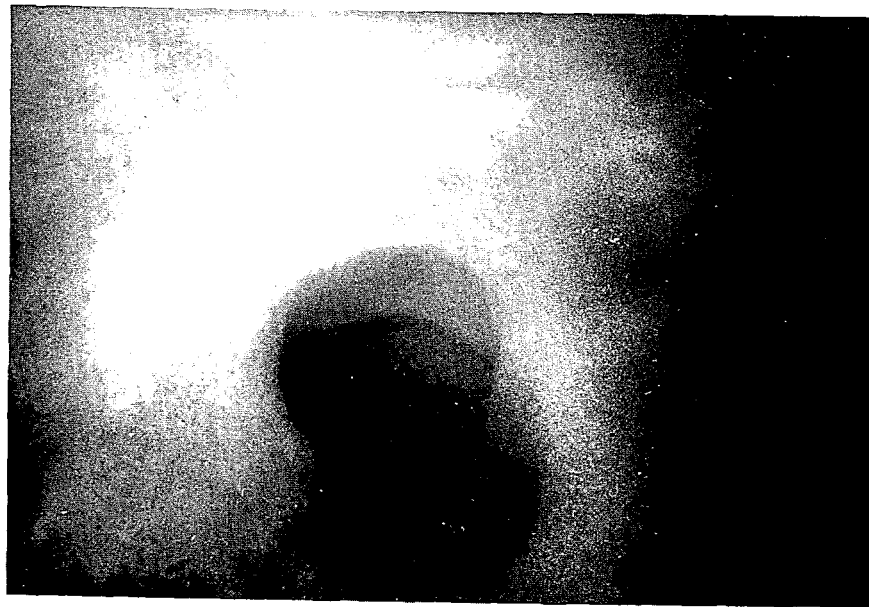


Fig. 8 — Photograph of two 50-cm auger holes in the pedestal. The distant hole exposes the sea floor and shows the narrow gap between sediments and the bottom of the ice island.

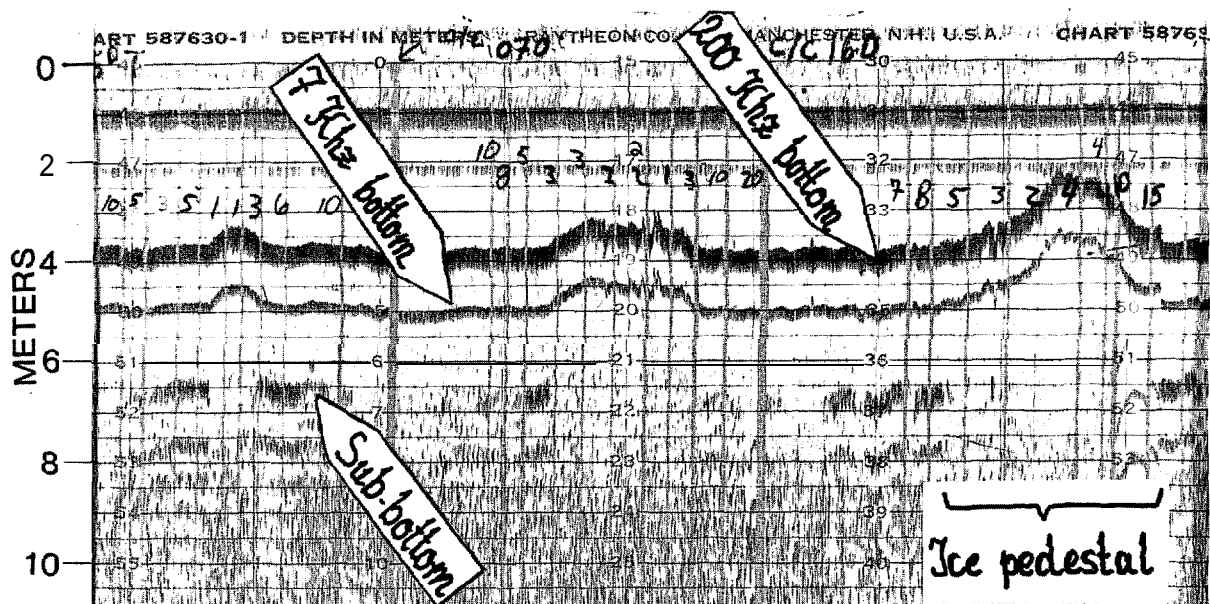


Fig. 9 — Fathometer and sub-bottom profiles recorded along short passes skirting the island. Courses and distances (m) to bluff are recorded. Note loss of sub-bottom reflector under pedestal.

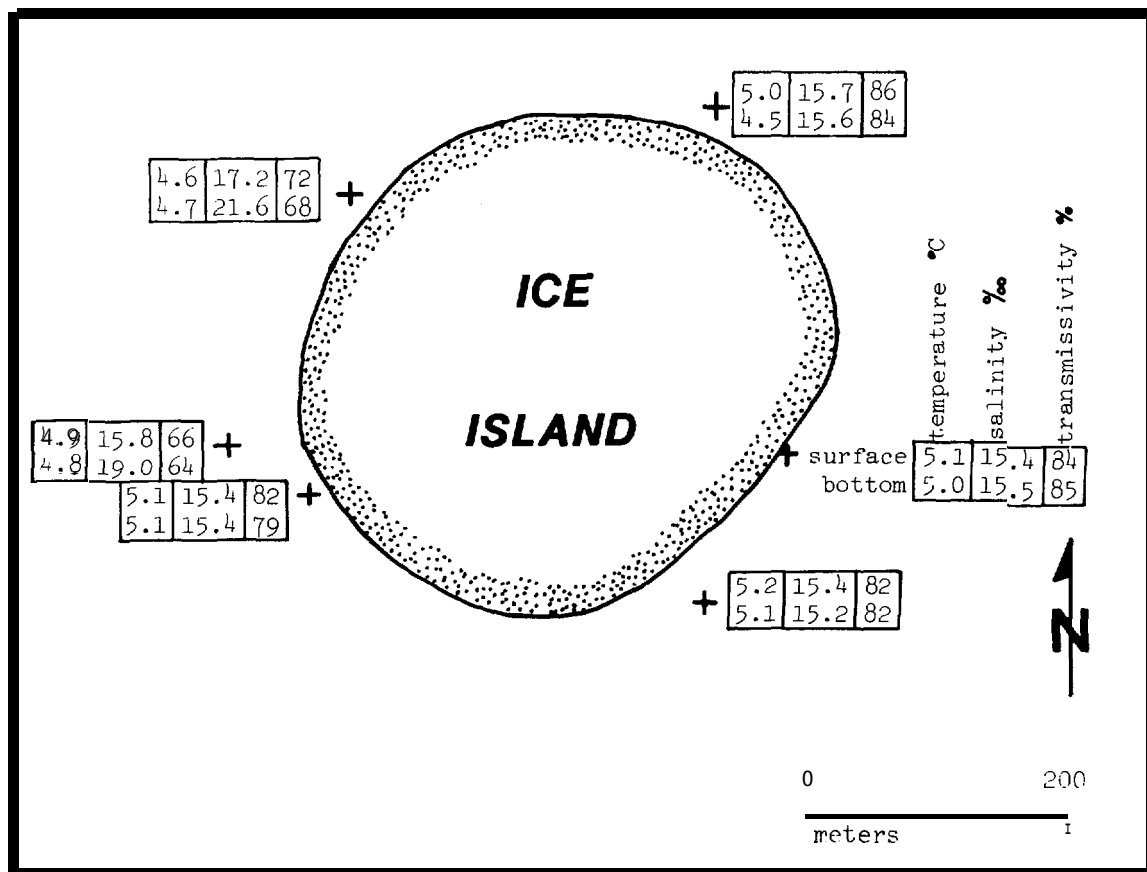


Fig. 10 — Surface and bottom measurements of water salinity, temperature, and transmissivity around island on 7-27, with winds from NE and westward currents. Outline of island as measured on that day.